

Photon Radiation and Dilepton Production Induced by Rescattering in Strong Interacting Medium

Hanzhong Zhang, Zhongbo Kang, Ben-Wei Zhang and Enke Wang
*Institute of Particle Physics, Huazhong Normal University, Wuhan 430079,
 China; Key Laboratory of Quark & Lepton Physics (HZNU), MOE, China*

Using the opacity expansion technique we investigate the photon radiation and dilepton production induced by multiple rescattering as energetic parton jet passing through the strong interacting medium. The real photon radiation and dilepton invariant-mass spectra of the bremsstrahlung contribution from an energetic quark jet are presented. The leading contribution of total energy loss by photon emission in medium of a higher energy quark jet is found to be proportional to the jet energy and has a linear dependence on the thickness of the nuclear target. The rescattering contribution for the dilepton is important only for small value of the invariant-mass and for the not so fast jet. The contribution fraction of the dilepton induced by rescattering in medium is found to be nearly a constant when the ratio of jet energy to Debye screening mass E/μ is large.

PACS numbers: 11.80.La, 12.38.Mh, 12.38.Bx, 25.75.Nq

I. INTRODUCTION

Hard processes are considered as a good tool to study the properties of the quark matter produced in ultra-relativistic heavy-ion collision because it can probe the early stage of the evolution of dense system, during which a quark-gluon plasma (QGP) could exist for a short period of time. One important aspect of hard processes is jet's energy loss or jet quenching [1, 2, 3, 4, 9, 10, 11, 12, 13] due to gluon radiation induced by multiple rescattering as energetic parton jet going through the strong interacting medium. Jet quenching in high energy nucleus-nucleus collisions is predicted to lead to strong suppression of both single- and correlated away-side dihadron spectra at large transverse momentum as compared to $p + p$ collisions at the same energy [1, 12, 13]. These phenomenon have been observed in central nucleus-nucleus collisions in recent RHIC experiments [14, 15, 16, 17, 18, 19, 20]. A simultaneous χ^2 -fit to both single and dihadron spectra can be achieved within their minima in the same narrow range of energy loss parameter for two different measurements at RHIC [13]. This fact provides convincing evidence for jet quenching description.

In addition to the gluon radiation, an energetic quark jet suffering multiple rescattering in medium should also induce real and virtual photon bremsstrahlung, where the emitted virtual photon may further decay into a dilepton. Since the (real or virtual) photon interacts with the particles in the collision region only through the electromagnetic coupling, its mean-free path is expected to be quite large[21]. One expects the photons can pass through the collision region without rescattering and then carry the information of medium at the time they have been produced, which may help us analyze the properties of the hot nuclear matter created in relativistic nucleus-nucleus collisions and provide complementary test of jet quenching mechanism due to gluon emission off their same parent jet[22, 23, 24].

The bremsstrahlung photon production in nucleus-nucleus collisions has been previously discussed by many researchers. B. G. Zakharov studied[24] the induced photon bremsstrahlung from a fast quark produced in $A + A$ collisions due to multiple scattering in QGP and predicted the medium- induced photon emission may enhanced the photon production at high p_T in $A + A$ collisions by 30% as compared to $p + p$ collisions, which is not consistent with the recent PHENIX measurements [25]. By using diagrammatic method in thermal field theory, Arnold, Moore and Yaffe (AMY)[26] calculated the photon and gluon emission rates of an equilibrated, hot QCD plasma to the leading order in both α_e and the QCD coupling $g_s(T)$, where the energy loss of an asymptotic jet in QGP is investigated by assuming a very high temperature to guarantee $g_s(T) \ll 1$. Later S. Turbide, C. Gale, S. Jeon and G. Moore (TGJM)[27] utilize AMY formalism to study high p_T pion and photon production including bremsstrahlung process in heavy-ion collisions at RHIC and LHC. However, their results overestimate the photon production at $Au + Au$ with $\sqrt{s_{NN}} = 200$ GeV measured by PHENIX experiments [25].

Therefore, it is interesting and beneficial to make an complementary calculation of photon production in $A + A$ collision with different approaches. In this paper we follow the framework of opacity expansion developed by Gyulass, Levai and Vitev (GLV) in Ref.[4] to study the bremsstrahlung photon and dilepton production induced by multiple rescattering as the parton jet propagating in the strong interacting medium. The GLV formalism has been extensively applied to study the high p_T phenomenon at RHIC and the phenomenological studies based on GLV formalism have described different measurements at RHIC very well [5, 6, 7]. In GLV formalism the contributions of radiative energy loss in expanded in powers of the opacity, which is defined as the averaged scattering number, L/λ with L representing the thickness of the target and λ the gluon mean-free path. And it has been shown that the opacity expansion series converge very rapidly and the first order contribution is dominant.

For the comparison of several jet quenching approaches including AMY and GLV formalism, please see the review in Ref.[8].

As a first step we concentrate on the production of photon and dilepton emitted off a fast quark jet at the first order opacity. In our calculation the QCD coupling g_s from the scattering point where a quark jet interacts with a parton in a QGP system, is put in a potential function and absorbed into opacity. Therefore, compared with AMY's study[26], our result of photon emission rate at first order opacity is also to the leading order in both α_e and α_s . Our conclusions about bremsstrahlung photon in strong interacting medium are qualitatively consistent with AMY's studies. We confirm that the leading contribution of energy loss by photon emission has a linear dependence on the thickness of the nuclear target L [28], which is different from the energy loss by gluon radiation where ΔE quadratically depend on the thickness L . We observe that the rate of photon radiation as a function of energy fraction x carried by radiated photon has a peak at small $x \sim 0.3$, whereas in Zakharov's study the peak of the rate by induced photon correction is at $x \sim 0.9$. This may explain why a larger enhancement factor of photon production at high p_T in $A + A$ is found in Zakharov's study. For a jet created in $A + A$ collisions, multiple scattering induces photon radiation as well as gluon radiation (jet quenching). Compared with the case of $p + p$ collisions, induced photon radiation enhances the photon yield while jet quenching decreases the photon yield from jet fragmentation in $A + A$ collisions[22, 23, 24]. If the former effect is overestimated larger than the latter effect, the nuclear modification factor for medium and large p_T photon production $R_{AA} > 1$ will appear in $A + A$ collisions, not consistent with the recent PHENIX measurements [25].

For dilepton production it is shown the rescattering contribution is important only for small value of the invariant-mass and also for the not so fast jet, and the contribution fraction of dilepton induced by multiple scattering to approach a constant when the quark jet energy $E/\mu > 30$, where E denotes the energy of the jet, and μ the debye screening mass.

This paper is organized as follows. In Sec. II we present the calculation of the jet energy loss by photon emission in hot medium and the resulting photon spectrum due to real photon radiation. In Sec. III we investigate the invariant-mass spectrum in the dilepton production due to virtual photon radiation. Corresponding numerical analysis are given in these two sections, respectively. In Sec. IV we make a brief conclusion.

II. INDUCED REAL PHOTON RADIATION

Consider a source localized at $y_0 = (t_0, \mathbf{y}_0)$ that produces a parton jet described by a wave packet $J(p)$. The parton jet undergoes multiple rescattering by exchanging a gluon with a target parton and emits a photon with

light-cone 4-momentum and polarization,

$$k = \left[xp^+, \frac{\mathbf{k}_\perp^2}{xp^+}, \mathbf{k}_\perp \right], \quad (1)$$

$$\epsilon = \left[0, \frac{2\epsilon_\perp \cdot \mathbf{k}_\perp}{xp^+}, \epsilon_\perp \right], \quad (2)$$

where x is the energy fraction carried by photon from the jet parton. The initial and final four momentum of the jet is assumed as

$$p_i = [p^+, p^-, 0_\perp], \quad (3)$$

$$p_f = \left[(1-x)p^+, \frac{(\mathbf{q}_\perp - \mathbf{k}_\perp)^2 + m^2}{(1-x)p^+}, \mathbf{q}_\perp - \mathbf{k}_\perp \right], \quad (4)$$

where \mathbf{q}_\perp and m denote the transverse momentum transfer and thermal mass of the jet parton in the hot medium, respectively.

As proposed by Gyulassy and Wang[1], the interaction between the jet and the target parton can be modeled by the static color-screened Yukawa potential,

$$V_n = 2\pi\delta(q^0)v(\mathbf{q}_n)e^{-i\mathbf{q}_n \cdot \mathbf{y}_n}T_{a_n}(j) \otimes T_{a_n}(n), \quad (5)$$

$$v(\mathbf{q}) = \frac{4\pi\alpha_s}{\mathbf{q}_n^2 + \mu^2}, \quad (6)$$

where α_s is the strong coupling constant, μ the Debye thermal mass of gluon in the hot medium, \mathbf{q}_n the momentum transfer from a target parton n at the coordinates $\mathbf{y}_n = (z_n, \mathbf{y}_\perp n)$. $T_{a_n}(j)$ and $T_{a_n}(n)$ are the color matrices for the jet and target parton, respectively. As assumed in Ref.[4], all target partons are in the same d_T dimensional representation with Casimir $C_2(T)$ ($TrT_a(n) = 0$ and $Tr(T_a(i)T_b(j)) = \delta_{ij}\delta_{ab}C_2(i)d_T/d_A$). For color matrices generators of the jet in the d_R dimensional representation, $Tr(T_a(j)T_a(j)) = C_R d_R$.

As shown in Fig.1, we denote \mathcal{M}_0 , \mathcal{M}_1 and \mathcal{M}_2 as the scattering amplitudes for self-quenching, single rescattering and the double Born rescattering, respectively. The squared total amplitude is given by

$$\begin{aligned} |\mathcal{M}_s|^2 &= |\mathcal{M}_0 + \mathcal{M}_1 + \mathcal{M}_2 + \dots|^2 \\ &= |\mathcal{M}_0|^2 + |\mathcal{M}_1|^2 + 2Re(\mathcal{M}_1\mathcal{M}_0^*) \\ &\quad + 2Re(\mathcal{M}_2\mathcal{M}_0^*) + \dots \end{aligned} \quad (7)$$

For the self-quenching shown in Fig.1 we get

$$\mathcal{M}_0 = iJ(p+k)e^{i(p+k) \cdot y_0} \mathcal{R}_0, \quad (8)$$

where the radiation amplitude \mathcal{R}_0 can be expressed as

$$\mathcal{R}_0 = g \frac{\epsilon \cdot k}{p \cdot k} = 2g(1-x) \frac{\epsilon_\perp \cdot \mathbf{k}_\perp}{\mathbf{k}_\perp^2 + x^2 m^2}, \quad (9)$$

g is the coupling constant between quark and photon.

For multiple rescattering we assume the packet $J(p)$ vary slowly over the range of momentum transfers supplied by the potential, the rescattering centers are well

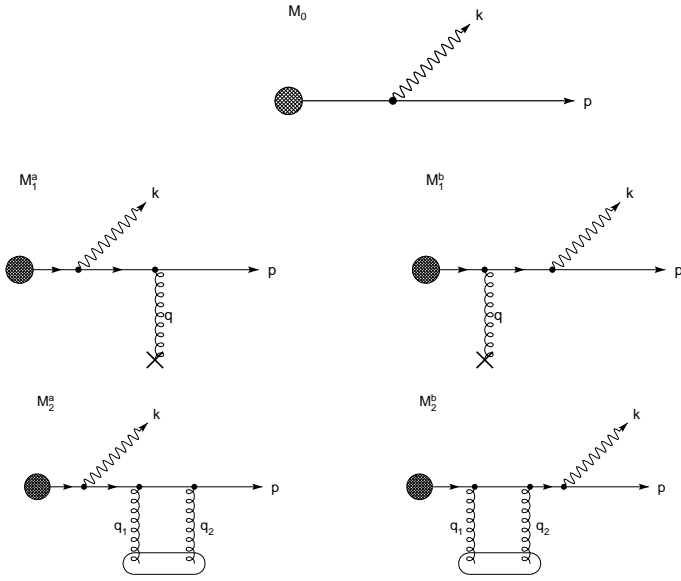


FIG. 1: Feynman diagram for photon radiation induced by self-quenching, single and double Born rescattering in the medium.

separated and the distance between two successive scattering is large compared to the interaction range,

$$z_i - z_{i-1} \gg 1/\mu. \quad (10)$$

For single scattering illustrated in Fig.1 the rescattering amplitude of the first Feynman diagram can be expressed as

$$\begin{aligned} \mathcal{M}_1^a &= iJ(p+k)e^{i(p+k)\cdot y_0} \sum_{j=1}^N \int \frac{d^2 \mathbf{q}_{\perp}}{(2\pi)^2} e^{-i\mathbf{q}_{\perp}\cdot(\mathbf{y}_{\perp j} - \mathbf{y}_{0\perp})} \\ &\times \int \frac{dq_z}{2\pi} \frac{2g(1-x)p^+\epsilon \cdot p_i}{[(p-q)^2 + i\epsilon][(p+k-q)^2 + i\epsilon]} \\ &\times v(q_z, \mathbf{q}_{\perp}) e^{-iq_z(z_j - z_0)} T_a T_a(j), \end{aligned} \quad (11)$$

where N is the number of the targets in the medium. The integration over q_z is performed by closing the contour below the real axis in the complex q_z plane. Two poles $q_z' = -i\epsilon$ and $q_z'' = -\omega_0 - i\epsilon$ contribute to the scattering amplitude. Here ω_0 can be written as

$$\omega_0 = \frac{\mathbf{k}_{\perp}^2 + x^2 m^2}{xp^+}. \quad (12)$$

The contribution from the pole corresponding to the potential singularities can be neglected because of the suppression factor $\exp[-\mu(z - z_0)]$. From Eq.(11) we deduce the radiation amplitude for first Feynman diagram of the single rescattering in Fig.1 as

$$\mathcal{R}_1^a = -i2g(1-x) \frac{\epsilon_{\perp} \cdot \mathbf{k}_{\perp}}{\mathbf{k}_{\perp}^2 + x^2 m^2} \sum_{j=1}^N \left[1 - e^{i\omega_0(z_j - z_0)} \right]. \quad (13)$$

Similarly we get the radiation amplitude for second Feynman diagram of the single rescattering in Fig.1 as

$$\begin{aligned} \mathcal{R}_1^b &= -i2g(1-x) \frac{\epsilon_{\perp} \cdot (\mathbf{k}_{\perp} - x\mathbf{q}_{\perp})}{(\mathbf{k}_{\perp} - x\mathbf{q}_{\perp})^2 + x^2 m^2} \\ &\times \sum_{j=1}^N e^{i\omega_0(z_j - z_0)}. \end{aligned} \quad (14)$$

Then the total radiation amplitude for single scattering is given by

$$\begin{aligned} \mathcal{R}_1 &= \mathcal{R}_1^a + \mathcal{R}_1^b = -i2g(1-x) \\ &\times \epsilon_{\perp} \cdot \sum_{j=1}^N \left[\mathbf{B} - (\mathbf{B} - \mathbf{C}) e^{i\omega_0(z_j - z_0)} \right], \end{aligned} \quad (15)$$

where

$$\mathbf{B} = \frac{\mathbf{k}_{\perp}}{\mathbf{k}_{\perp}^2 + x^2 m^2}, \quad \mathbf{C} = \frac{\mathbf{k}_{\perp} - x\mathbf{q}_{\perp}}{(\mathbf{k}_{\perp} - x\mathbf{q}_{\perp})^2 + x^2 m^2}. \quad (16)$$

For the double Born virtual interaction shown in Fig.1, $y_1 = y_2 = y_j$, the rescattering amplitude \mathcal{M}_2^a reads

$$\begin{aligned} \mathcal{M}_2^a &= iJ(p+k)e^{i(p+k)\cdot y_0} \sum_{j=1}^N \int \frac{d^2 \mathbf{q}_{1\perp}}{(2\pi)^2} \int \frac{d^2 \mathbf{q}_{2\perp}}{(2\pi)^2} \\ &\times e^{-i(\mathbf{q}_{1\perp} + \mathbf{q}_{2\perp}) \cdot (\mathbf{y}_{\perp j} - \mathbf{y}_{\perp 0})} (1-x)^2 p^{+2} \int \frac{dq_{2z}}{2\pi} \\ &\times v(\mathbf{q}_{2\perp}) T_{a_2} T_{a_2}(j) \Delta(p - q_2) \int \frac{dq_{1z}}{2\pi} v(\mathbf{q}_{1\perp}) T_{a_1} T_{a_1}(j) \\ &\times e^{-i(q_{1z} + q_{2z})(z_j - z_0)} 2g[\epsilon \cdot (p - q_1 - q_2)] \\ &\times \Delta(p - q_1 - q_2) \Delta(p + k - q_1 - q_2). \end{aligned} \quad (17)$$

Integrate over q_{1z} by closing the contour below the real axis in the complex q_{1z} plane, the residue of the poles $q_{1z}' = -q_{2z} - i\epsilon$ and $q_{1z}'' = -q_{2z} - \omega_0 - i\epsilon$ contribute to the integral. The contribution from the potential singularities can be ignored because $z_j - z_0 \gg 1/\mu$. so \mathcal{M}_2^a can be rewritten as

$$\begin{aligned} \mathcal{M}_2^a &= iJ(p+k)e^{i(p+k)\cdot y_0} \sum_{j=1}^N \int \frac{d^2 \mathbf{q}_{1\perp}}{(2\pi)^2} \int \frac{d^2 \mathbf{q}_{2\perp}}{(2\pi)^2} \\ &\times e^{-i(\mathbf{q}_{1\perp} + \mathbf{q}_{2\perp}) \cdot (\mathbf{y}_{\perp j} - \mathbf{y}_{\perp 0})} (1-x)^2 p^{+2} \int \frac{dq_{2z}}{2\pi} \\ &\times \frac{-2ig}{\omega_0(1-x)p^{+2}} v(q_{2z}, \mathbf{q}_{2\perp}) v(-q_{2z}, \mathbf{q}_{1\perp}) \Delta(p - q_2) \\ &\times \epsilon \cdot p_i \left[1 - e^{i\omega_0(z_j - z_0)} \right] T_{a_1} T_{a_1}(j) T_{a_2} T_{a_2}(j). \end{aligned} \quad (18)$$

For q_{2z} integration, there is no exponentially suppressed factor, so the potential singularities $q_{2z} = -i\mu_1$ and $-i\mu_2$ contribute to the integral. By closing the integration contour below the real axis in the complex q_{2z} plane and taking the residue in the poles $q_{2z} = -i\epsilon$ and $q_{2z}'' = -i\sqrt{\mathbf{q}_{2\perp}^2 + \mu^2}$, we get the radiation amplitude

$$\mathcal{R}_2^a(\text{Born}) = -g(1-x) \epsilon_{\perp} \cdot \mathbf{B} \sum_{j=1}^N \left[1 - e^{i\omega_0(z_j - z_0)} \right]. \quad (19)$$

In a similar way, from the last Feynman diagram in Fig. 1 we obtain the rescattering amplitude \mathcal{M}_2^b . The corresponding radiation is given by

$$\mathcal{R}_2^b(\text{Born}) = -g(1-x)\epsilon_{\perp} \cdot \mathbf{B} \sum_{j=1}^N e^{i\omega_0(z_j-z_0)}. \quad (20)$$

The total radiation amplitude from the double Born virtual interaction can be expressed as

$$\begin{aligned} \mathcal{R}_2^B &= \mathcal{R}_2^a(\text{Born}) + \mathcal{R}_2^b(\text{Born}) \\ &= -g(1-x)N\epsilon_{\perp} \cdot \mathbf{B}. \end{aligned} \quad (21)$$

As shown in Ref.[4], in opacity expansion technique we make following simplification: define the relative transverse coordinate $\mathbf{b}_{\perp j} = \mathbf{y}_{\perp j} - \mathbf{y}_{\perp 0}$, it varies over a large transverse area A_{\perp} . Then the ensemble average over the rescattering center location reduces to an impact parameter average,

$$\langle \dots \rangle = \frac{1}{A_{\perp}} \int d^2\mathbf{b}_{\perp} dz_j dz_0 \rho(z_j, z_0) \dots \quad (22)$$

Along the longitudinal direction, the distribution density for the locations of the rescattering center is defined by

$$\begin{aligned} \rho(z_0, z) &= \left[\frac{\theta(L-z)}{L/2} \text{Exp}\left(-\frac{L-z}{L/2}\right) \right] \\ &\times \left[\frac{\theta(z-z_0)}{L/2} \text{Exp}\left(-\frac{z-z_0}{L/2}\right) \right]. \end{aligned} \quad (23)$$

Taking the initial color average and the ensemble average we obtain

$$\begin{aligned} \langle |\mathcal{M}_1|^2 \rangle &= \int dz_0 dz \rho(z_0, z) \frac{N\sigma_{el}}{A_{\perp}} \\ &\times \int d^2\mathbf{q}_{\perp} \frac{1}{\sigma_{el}} \frac{C_R C_2(T)}{d_A} \frac{|v(0, \mathbf{q}_{\perp})|^2}{(2\pi)^2} |\mathcal{R}_1|^2 \end{aligned} \quad (24)$$

The elastic cross section with the small transverse momentum transfer between the jet and target partons is [1, 4]

$$\frac{d\sigma_{el}}{d^2\mathbf{q}_{\perp}} = \frac{C_R C_2(T)}{d_A} \frac{|v(0, \mathbf{q}_{\perp})|^2}{(2\pi)^2}. \quad (25)$$

One can defining $|\bar{v}(0, \mathbf{q}_{\perp})|^2$ as the normalized distribution of momentum transfers from the scattering centers[4],

$$\frac{1}{\sigma_{el}} \frac{d\sigma_{el}}{d^2\mathbf{q}_{\perp}} \equiv |\bar{v}(0, \mathbf{q}_{\perp})|^2 = \frac{1}{\pi} \frac{\mu_{eff}^2}{(\mathbf{q}_{\perp}^2 + \mu^2)^2}, \quad (26)$$

where

$$\frac{1}{\mu_{eff}^2} = \frac{1}{\mu^2} - \frac{1}{\mu^2 + \mathbf{q}_{\perp}^2}, \quad (27)$$

to insure $\int^{\mathbf{q}_{\perp max}} d^2\mathbf{q}_{\perp} |\bar{v}(0, \mathbf{q}_{\perp})|^2 = 1$. In numerical estimation, we take that $\mathbf{q}_{\perp max}^2 = \infty$, $\mu_{eff} \approx \mu$.

Using the normalized distribution $|\bar{v}(0, \mathbf{q}_{\perp})|^2$, we can rewrite Eq.(24) as

$$\begin{aligned} \langle |\mathcal{M}_1|^2 \rangle &= \frac{L}{\lambda} \int d^2\mathbf{q}_{\perp} |\bar{v}(0, \mathbf{q}_{\perp})|^2 \\ &\times \int dz_0 dz \rho(z_0, z) |\mathcal{R}_1|^2, \end{aligned} \quad (28)$$

where

$$\frac{L}{\lambda} = \frac{N\sigma_{el}}{A_{\perp}} \equiv \bar{n}. \quad (29)$$

\bar{n} represents the mean number of the rescattering which is defined as the so-called opacity[4].

The first interference term $Re(\mathcal{M}_1 \mathcal{M}_0^*)$ in Eq.(7) doesn't contribute to photon radiation probability because of $Tr(T_a(j)) = 0$. The contribution from the double Born virtual interaction is given by

$$\begin{aligned} \langle 2Re(\mathcal{M}_2^B \mathcal{M}_0^*) \rangle &= \frac{L}{\lambda} \int d^2\mathbf{q}_{\perp} |\bar{v}(0, \mathbf{q}_{\perp})|^2 \\ &\times \int dz_0 dz \rho(z_0, z) 2Re(\mathcal{R}_2^B \mathcal{R}_0^*). \end{aligned} \quad (30)$$

Denote N as the number of the radiated photon, we have

$$dN = \langle |\mathcal{M}|^2 \rangle \frac{d^3\mathbf{k}}{(2\pi)^3 2\omega}. \quad (31)$$

The transverse momentum spectrum of the radiated photon can be expressed as

$$\frac{dN}{d|\mathbf{k}_{\perp}|^2 dx} = \frac{1}{4(2\pi)^2} \frac{1}{x} \langle |\mathcal{M}|^2 \rangle. \quad (32)$$

To the first order of opacity expansion, the square of the rescattering amplitude is given by

$$\begin{aligned} \langle |\mathcal{M}|^2 \rangle &= \langle |\mathcal{M}_0|^2 + |\mathcal{M}_1|^2 + 2Re(\mathcal{M}_2^B \mathcal{M}_0^*) \rangle \\ &= |\mathcal{R}_0|^2 + \frac{L}{\lambda} \int \frac{\mu^2 d^2\mathbf{q}_{\perp}}{\pi(\mathbf{q}_{\perp}^2 + \mu^2)^2} \int dz_0 dz \\ &\times \rho(z_0, z) [|\mathcal{R}_1|^2 + 2Re(\mathcal{R}_2^B \mathcal{R}_0^*)], \end{aligned} \quad (33)$$

where

$$\begin{aligned} |\mathcal{R}_1|^2 &+ 2Re(\mathcal{R}_2^B \mathcal{R}_0^*) = 4g^2(1-x)^2[(\mathbf{B} - \mathbf{C})^2 \\ &- 2\cos(\omega_0(z-z_0))(\mathbf{B}^2 - \mathbf{B} \cdot \mathbf{C})]. \end{aligned} \quad (34)$$

The term with $\cos(\omega_0(z-z_0))$ reflects the destructive interference arising from the Abelian LPM effect[29]. The integration of this term over target distribution gives

$$\begin{aligned} I(\omega_0, L) &\equiv \int dz_0 dz \rho(z_0, z) \cos(\omega_0(z-z_0)) \\ &= \frac{4}{4 + \omega_0^2 L^2}. \end{aligned} \quad (35)$$

Denote $dN_{0+1} = dN_0 + dN_1$, N_0 is the number of radiated photon at zero-order opacity expansion corresponding to self-quenching term $|\mathcal{M}_0|^2$, N_1 the number of radiated photon at first-order opacity expansion corresponding to the sum of single rescattering term $|\mathcal{M}_1|^2$ and the interference term between self-quenching and double born virtual interaction $2Re(\mathcal{M}_2^B \mathcal{M}_0^*)$. Defining

$$u = |\mathbf{q}_\perp|^2/\mu^2, \quad y = |\mathbf{k}_\perp|^2/\mu^2, \quad w = m^2/\mu^2, \quad (36)$$

we obtain

$$\frac{dN_0}{dxdy} = \frac{4\alpha_e}{9\pi} \frac{(1-x)^2}{x} \frac{y}{(y+x^2w)^2}, \quad (37)$$

$$\frac{dN_1}{dxdy} = \frac{4\alpha_e}{9\pi} \frac{(1-x)^2}{x} \frac{L}{\lambda} \int du \frac{1}{(1+u)^2} f(x, u, y), \quad (38)$$

where function $f(x, u, y)$ is given by

$$f(x, u, y) = \frac{(y+x^2u)(y+x^2w+x^2u) - 4x^2uy}{\sqrt{((y+x^2u+x^2w)^2 - 4x^2uy)^3}} - \frac{y}{(y+x^2w)^2} + (1 - I(\omega_0, L)) \frac{1}{y+x^2w} \times \left(\frac{y-x^2w}{y+x^2w} - \frac{y-x^2w-x^2u}{\sqrt{(y+x^2u+x^2w)^2 - 4x^2uy}} \right). \quad (39)$$

In getting above expressions the integral of the angle between \mathbf{k}_\perp and \mathbf{q}_\perp has been integrated out and we have chosen the coupling constant $g = 2e/3$ for u light quark jet.

If setting the mass of quark to vanish, from Eq.(36) we see $w = 0$, then function $f(x, u, y)$ in Eq.(39) reduce to

$$f(x, u, y) = \frac{1}{|y-x^2u|} - \frac{1}{y} + (1 - I(\omega_0, L)) \frac{1}{y} \left(1 - \frac{y-x^2u}{|y-x^2u|} \right). \quad (40)$$

This function have two collinear divergences. One is from the initial-state bremsstrahlung as $y \sim 0$ (or $\mathbf{k}_\perp \sim 0$) along the initial jet direction; the another one is from the final-state bremsstrahlung along the final jet direction as $|\mathbf{k}_\perp| \sim x|\mathbf{q}_\perp|$ (or emission angle θ_e is near to the scattering angle θ_s), here θ_e and θ_s approximate

$$\theta_e \sim \frac{|\mathbf{k}_\perp|}{k^+}, \quad \theta_s \sim \frac{|\mathbf{q}_\perp|}{p^+}. \quad (41)$$

Above two collinear divergences is caused by setting quark jet's mass to be zero. As $\theta_e > \theta_s$, the third term in Eq.(40) vanish, so there is no interference. In purely QED case, as $\theta_e < \theta_s$ the radiative energy loss of the charged particle has been studied in Ref.[30] in which the charged particle undergoes multiple rescattering by exchanging photon. Here we investigate the transverse

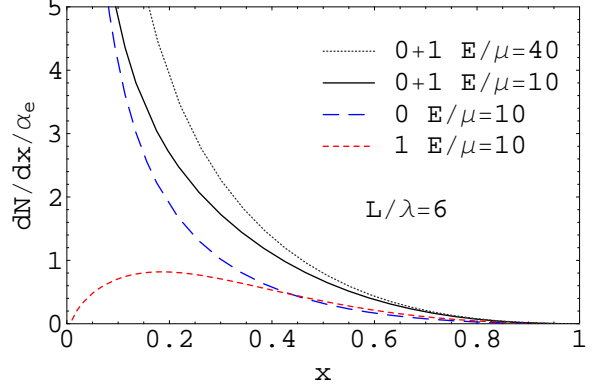


FIG. 2: (Color online) The production rates of the photon emitted off two quark jets with energy $E/\mu = 10, 40$, respectively. The upper two curves (the dot for the jet with energy $E/\mu = 40$, the solid for the jet with energy $E/\mu = 10$) are for the contributions to the first order opacity (denoted as “0+1”). The long-dashed curve is for the self-quenching contribution (denoted as “0”) from the jet with $E/\mu = 10$ while the short-dashed curve for the induced contribution (denoted as “1”) from the same jet at the first order opacity. The opacity is chosen as $L/\lambda = 6$.

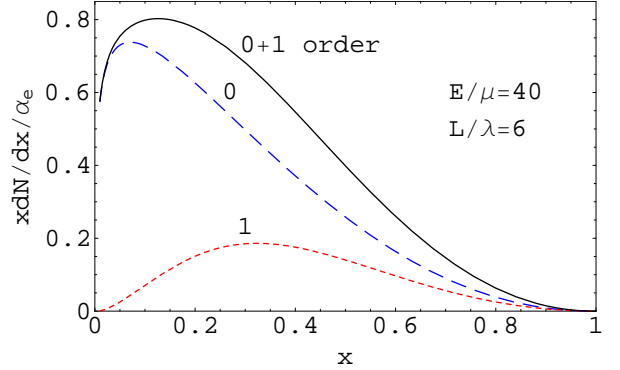


FIG. 3: (Color online) The radiation rate of the electromagnetic energy from a energy-given quark jet by radiating photons carrying energy fraction x of the jet.

momentum spectrum of radiated photon and the corresponding energy loss of energetic quark jet which undergoes multiple rescattering by exchanging gluon.

To avoid the collinear divergences, in the following we take the thermal mass of quark and gluon from “hard thermal loops”[31] as

$$m^2 = \frac{g_s^2 C_F T^2}{8}, \quad (C_F = \frac{4}{3}), \quad (42)$$

$$\mu^2 = (N_c + \frac{N_f}{2}) \frac{g_s^2 T^2}{9}, \quad (43)$$

where N_c and N_f are the number of the color and flavor of quark, respectively. After taking into account the thermal mass of quark, the collinear divergences in Eq.(39) disappear. In following numerical calculation, we will

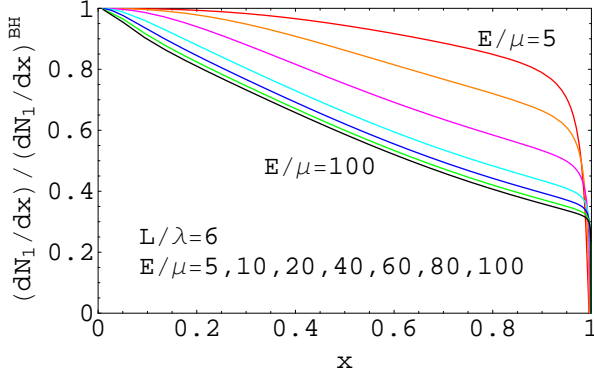


FIG. 4: (Color online) The ratio between the rescattering contribution at the first order opacity and that of corresponding BH-limit for a quark jet with different energies.

choose $\mu = 0.5\text{GeV}$ given by Eq.(43), the mean free path $\lambda = 1\text{fm}$, and consider the kinetic limits of the photon's transverse momentum[10],

$$\mu^2 \leq \mathbf{k}_\perp^2 \leq 4E^2x(1-x). \quad (44)$$

Shown in Fig.2 is the production rates of the photon emitted off two energy-given quark jets, respectively. The total photon production rate (“0+1” order opacity) decrease with the increasing photon energy (xE) and increases with the increasing jet energy. The variation tendency of the total rate is the same as AMY and TGJM's studies on bremsstrahlung contribution [26, 27]. Shown in Fig.3 is the radiation rate of the electromagnetic energy from a energy-given quark jet by radiating photons carrying energy fraction x of the jet. The variation tendency of the radiation rate is also similar to that of AMY's studies on bremsstrahlung contribution. Of interest is that our “0” and “1” order results can be directly compared with the “vacuum” and the “induced” contributions in Zakharov's studies, respectively. As $\mu = 0.5\text{GeV}$ is chosen in Eq.(43), the jet energy shown in Fig. 3 has a value $E = 20\text{GeV}$ same as an example in Zakharov's studies [24]. The variation tendency of our “0” order contribution is similar to that of “vacuum” contribution in Zakharov's studies. However, the peak of “1” order correction contribution is at $x = 0.3$ in our study while the peak of “induced” correction contribution is at $x = 0.9$ for finite kinematic boundaries in Zakharov's studies. For a jet created in $A + A$ collisions, multiple scattering induces photon radiation as well as gluon radiation (jet quenching). Compared with the case of $p + p$ collisions, induced photon radiation enhances the photon yield while jet quenching decreases the photon yield from jet fragmentation in $A + A$ collisions. If the former effect is estimated smaller than the latter effect, the nuclear modification factor for medium p_T photon production $R_{AA} < 1$ could be expected in $A + A$ collisions, close to experiment findings[25]. Our result for induced photon contribution smaller than that in

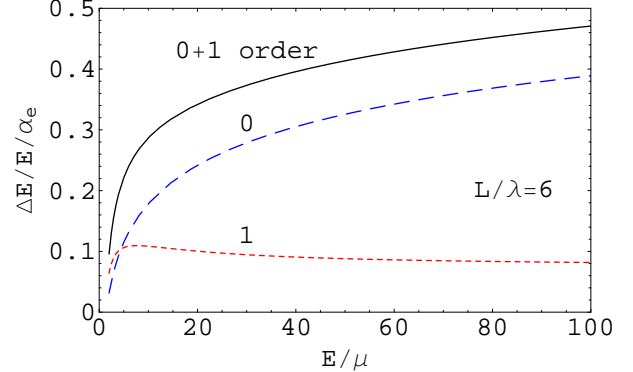


FIG. 5: (Color online) The total electromagnetic energy loss as a function of the energy of a quark jet.

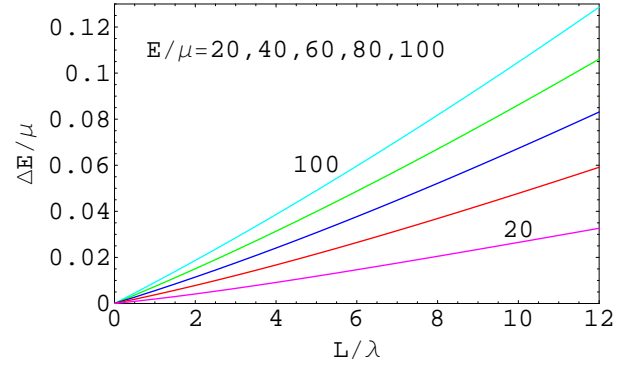


FIG. 6: (Color online) The total electromagnetic energy loss of a quark jet ($E/\mu = 5 - 100$) as a function of the thickness of the strong interaction medium.

Zakharov's study may explain why a too larger enhancement factor of photon production at high p_T in $A + A$ is found in Zakharov's study.

It is the same as pointed out in Ref.[1], from the relative phase factor $\omega_0(z - z_0)$ in Eq.(34) we define the formation time of the photon radiation as

$$\tau \equiv \frac{1}{\omega_0} = \frac{xp^+}{\mathbf{k}_\perp^2 + x^2m^2}. \quad (45)$$

When $z - z_0 \gg \tau$, the photon radiation reach the Bethe-Heitler (BH) limit in which the intensity of the induced radiation is additive in the number of rescattering. The BH-limit corresponds to $I(\omega_0, L) = 0$ in Eq.(35). Shown in Fig.4 are the ratio between the rescattering contribution at the first order opacity and that of corresponding BH-limit for a quark jet with different energies, $E/\mu = 5 - 100$. From Fig.4 we see that, at fixed jet energy, as x approaches small value, τ becomes small, the BH-limit is approached; at fixed x , as E/μ becomes small, τ becomes also small (in Eq.(45), $p^+ \sim 2E$), the BH-limit is achieved again.

Integrating over x in Fig.3 with different value of the

quark jet energy,

$$\Delta E/E = \int x dx \int d\mathbf{k}_\perp^2 \frac{dN}{d\mathbf{k}_\perp^2 dx}. \quad (46)$$

we obtain the total electromagnetic energy loss as a function of the energy of a quark jet, shown in Fig.5. For a fixed target thickness $L/\lambda = 6$, the self-quenching contribution increases with the increasing jet energy while the rescattering contribution (“1” order opacity correction) is almost a constant $\Delta E/E/\alpha_e = 0.1$ when $E/\mu > 5\text{GeV}$. It shows that for a high p_T quark jet the leading contribution of the total induced electromagnetic energy loss is proportional to the jet energy. Shown in Fig.6 is the total electromagnetic energy loss of a quark jet ($E/\mu = 5-100$) as a function of the thickness of the strong interaction medium. It is clear that the leading contribution of energy loss by photon emission has a linear dependence on the thickness of the nuclear target, which is different from the energy loss by gluon radiation where ΔE quadratically depend on the thickness L [4, 10]. Similar results are also observed in Ref.[28].

III. THE INDUCED DILEPTON PRODUCTION

What we study in above section is the real photon radiation when an energetic parton jet produced in heavy ion collisions propagates inside the strong interacting medium. If the radiative photon induced by multiple rescattering in above process is virtual, the virtual photon can decay into a lepton pair ($l\bar{l}$). In this section we investigate the induced dilepton production.

The Feynman diagram for dilepton production induced by self-quenching, single and double Born rescattering in the medium is shown in Fig.6. The amplitude for the dilepton radiation reads

$$\mathcal{M} = C_\mu \frac{-ig^{\mu\nu}}{k^2} \bar{u}(l^+) (-ie\gamma_\nu) u(l^-), \quad (47)$$

$$|\mathcal{M}|^2 = \frac{e^2}{k^4} W^{\mu\nu} L_{\mu\nu}, \quad (48)$$

where

$$W^{\mu\nu} = C^\mu C^{\nu*}, \quad (49)$$

$$L_{\mu\nu} = 4(l_\mu^+ l_\nu^- + l_\mu^- l_\nu^+ - l^+ \cdot l^- g_{\mu\nu}), \quad (50)$$

and C^μ is relate to the radiation amplitude for the virtual photon.

The invariant-mass spectrum for dilepton production can be expressed as

$$\frac{dN}{dM^2} = \frac{\alpha_e}{3\pi M^2} (-g_{\mu\nu} W^{\mu\nu}) \frac{d^3\mathbf{k}}{(2\pi)^3 2k^0}, \quad (51)$$

where $k^2 = M^2$, M is the invariant mass of the dilepton.

For virtual massive photon field, we can choose its polarization vector ϵ to satisfy $\epsilon \cdot k = 0$. Correspondingly

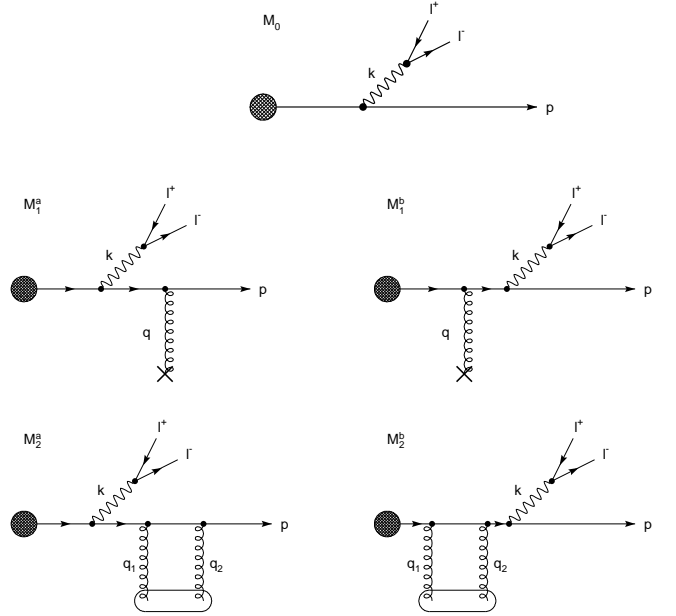


FIG. 7: Feynman diagram for dilepton production induced by self-quenching, single and double Born rescattering in the medium.

we have[32]

$$\sum_\lambda \epsilon_\mu(\lambda) \epsilon_\nu^*(\lambda) = -g_{\mu\nu} + \frac{k_\mu k_\nu}{M^2}. \quad (52)$$

Then we obtain

$$\begin{aligned} -g_{\mu\nu} W^{\mu\nu} &= \sum \left(\epsilon_\mu \epsilon_\nu^* C^\mu C^{\nu*} - \frac{k_\mu k_\nu^* C^\mu C^{\nu*}}{M^2} \right) \\ &= \sum \left(|\epsilon_\mu C^\mu|^2 - \frac{|k_\mu C^\mu|^2}{M^2} \right) \\ &= \sum |\epsilon_\mu C^\mu|^2. \end{aligned} \quad (53)$$

In getting last equality the Ward Identity has been used.

As an approximation, we consider a massless quark jet and assume $p^+ \gg k^+ \gg M$. From Eqs.(51) and (53) we see that $\epsilon_\mu C^\mu$ is the radiation amplitude for a on-shell virtual photon with mass M reduced by rescattering. Its calculation is very similar to the calculation of the radiation amplitude for a massless real photon in Sec.II, the only difference is that the light-cone 4-momentum in Eq.(1) should be replaced by

$$k = \left[xp^+, \frac{\mathbf{k}_\perp^2 + M^2}{xp^+}, \mathbf{k}_\perp \right]. \quad (54)$$

For self-quenching, single and double Born rescattering, the radiation amplitude of the virtual photon with mass M can be deduced as

$$\mathcal{R}'_0 = 2(1-x)g\epsilon_\perp \cdot \mathbf{B}', \quad (55)$$

$$\begin{aligned} \mathcal{R}'_1 &= -2ig(1-x) \\ &\times \epsilon_{\perp} \cdot \sum_{j=1}^N [\mathbf{B}' - (\mathbf{B}' - \mathbf{C}') e^{i\omega'_0(z_j - z_0)}], \end{aligned} \quad (56)$$

$$\mathcal{R}'_2^B = -(1-x)gN\epsilon_{\perp} \cdot \mathbf{B}', \quad (57)$$

where

$$\mathbf{B}' = \frac{\mathbf{k}_{\perp}}{\mathbf{k}_{\perp}^2 + M^2}, \quad \mathbf{C}' = \frac{\mathbf{k}_{\perp} - x\mathbf{q}_{\perp}}{(\mathbf{k}_{\perp} - x\mathbf{q}_{\perp})^2 + M^2}, \quad (58)$$

and

$$\omega'_0 = \frac{\mathbf{k}_{\perp}^2 + M^2}{xp^+}. \quad (59)$$

Correspondingly, the square of the radiation amplitude for the virtual photon to the first order in opacity expansion can be expressed as

$$\begin{aligned} -g_{\mu\nu}W^{\mu\nu} &= |\mathcal{R}'_0|^2 + \frac{L}{\lambda} \int \frac{\mu^2 d^2 \mathbf{q}_{\perp}}{\pi(\mathbf{q}_{\perp}^2 + \mu^2)^2} \\ &\times \int dz_0 dz \rho(z_0, z) [|\mathcal{R}'_1|^2 + 2\text{Re}(\mathcal{R}'_2^B \mathcal{R}'_0^*)] \end{aligned} \quad (60)$$

where

$$\begin{aligned} |\mathcal{R}'_1|^2 + 2\text{Re}(\mathcal{R}'_2^B \mathcal{R}'_0^*) &= 4g^2(1-x)^2[(\mathbf{B}' - \mathbf{C}')^2 \\ &- 2\cos(\omega'_0(z - z_0))(\mathbf{B}'^2 - \mathbf{B}' \cdot \mathbf{C}')] \end{aligned} \quad (61)$$

It is the same as in Eq.(34), the term with $\cos(\omega'_0(z - z_0))$ represents the destructive interference resulting from the Abelian LPM effect[29].

Substituting Eq.(60) into Eq.(51), we can obtain the invariant-mass spectrum arising from self-quenching at zero order in opacity,

$$\frac{dN_0}{dxdydw} = \frac{4\alpha_e^2}{27\pi^2} \frac{(1-x)^2}{xw} \frac{y}{(y+w)^2}, \quad (62)$$

and the invariant-mass spectrum arising from single and double Born rescattering at first order in opacity,

$$\begin{aligned} \frac{dN_1}{dxdydw} &= \frac{4\alpha_e^2}{27\pi^2} \frac{(1-x)^2}{xw} \frac{L}{\lambda} \\ &\times \int du \frac{1}{(1+u)^2} f(x, u, y, w), \end{aligned} \quad (63)$$

where function

$$\begin{aligned} f(x, u, y, w) &= \frac{(y+x^2u)(y+w+x^2u) - 4x^2uy}{\sqrt{((y+x^2u+w)^2 - 4x^2uy)^3}} \\ &- \frac{y}{(y+w)^2} + (1 - I(\omega'_0, L)) \frac{1}{y+w} \\ &\times \left(\frac{y-w}{y+w} - \frac{y-w-x^2u}{\sqrt{(y+x^2u+w)^2 - 4x^2uy}} \right) \end{aligned} \quad (64)$$

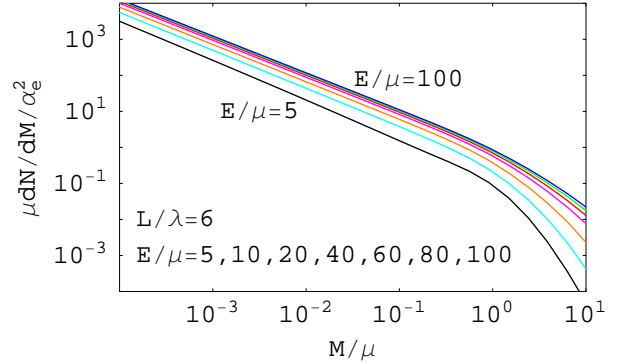


FIG. 8: (Color online) The invariant-mass spectra (“0+1” order) of the dilepton emitted off quark jets with different energies, $E/\mu = 5, 10, 20, 40, 60, 80, 100$, passing through the medium with the thickness, $L/\lambda = 6$.

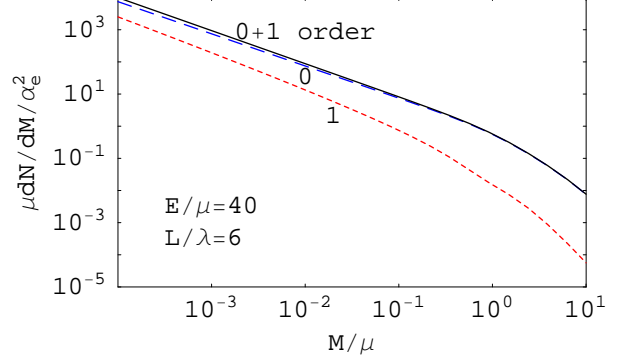


FIG. 9: (Color online) The comparison of the induced contribution (denoted as “1 order”) and the self-quenching contribution (denoted as “0”) of the invariant-mass spectra of the dilepton emitted off an energy-given quark jet, $E/\mu = 40$, passing through the medium with the thickness, $L/\lambda = 6$.

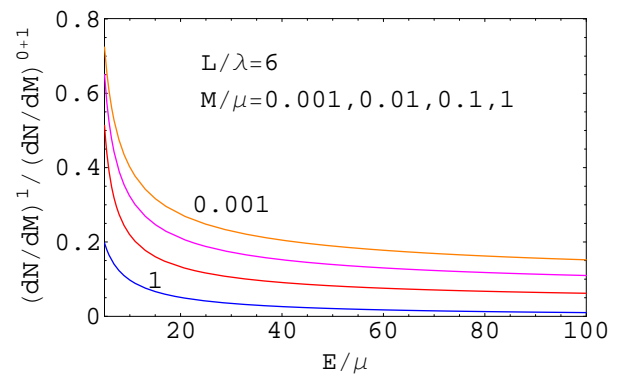


FIG. 10: (Color online) The ratio of the invariant-mass spectra between 1-order and (0+1)-order in opacity expansion. The invariant-mass is chosen as $M/\mu = 0.001, 0.01, 0.1, 1$, respectively.

and

$$u = |\mathbf{q}_\perp|^2/\mu^2, \quad y = |\mathbf{k}_\perp|^2/\mu^2, \quad w = M^2/\mu^2. \quad (65)$$

Shown in Fig.8 is the total invariant-mass spectra (“0+1” order opacity) of the dilepton emitted off quark jets with different energies, $E/\mu = 5, 10, 20, 40, 60, 80, 100$, passing through a target with the thickness, $L/\lambda = 6$. The invariant-mass spectrum decreases with the increasing invariant-mass while increases with the increasing jet energy. Shown in Fig.9 is the comparison of the induced contribution (“1 order” opacity) and the self-quenching contribution (“0” opacity) of the invariant-mass spectra of the dilepton emitted off an energy-given quark jet. For a jet with energy $E/\mu = 40$, the rescattering contribution is very small and can be neglected in the large invariant-mass region (especially when $M/\mu > 1$). In order to know clearly how much the rescattering contribution is in the total contribution, we plot Fig.10 to check the ratio of the invariant-mass spectra as a function of the jet energy between 1-order and (0+1)-order in opacity expansion. The invariant-mass is chosen as $M/\mu = 0.001, 0.01, 0.1, 1$, respectively. The plot demonstrates that the dilepton production induced by rescattering is important for small value of the invariant-mass and also the jet energy. In addition, the contribution fraction by rescattering is found to be nearly a constant when $E/\mu > 30$.

IV. CONCLUSION

In this paper we apply GLV’s opacity expansion technique to investigate the induced photon radiation and dilepton production in strong interacting medium. The real photon radiation and the dilepton invariant-mass spectrums are presented to the first order in opacity expansion. Our study focuses on the electromagnetic bremsstrahlung of an energy-given quark jet passing a thickness-given QGP system and the analytical derivation is combined with numerical calculation.

We show that for real photon radiation due to Abelian LPM effect the parton jet’s energy loss has a linear

dependence on the thickness of the targets instead of quadratic dependence arising from non-Abelian LPM effect for gluon radiation. And the leading contribution of the total induced electromagnetic energy loss of a fast quark is proportional to the jet energy.

The dilepton production by the decay from the virtual photon off a quark jet induced by multiple rescattering in medium has been investigated. It is shown that the invariant-mass spectrum decreases with the increasing invariant-mass while increases with the increasing jet energy. The rescattering contribution is important for small value of the invariant-mass and also for the not so fast jet. In addition, the contribution fraction by rescattering is found to be nearly a constant when the quark jet energy $E/\mu > 30$.

Of course, the study presented here is just the first step for photon and dilepton production in medium. To make a complete study of photon and dilepton production in $A + A$ collisions many other contributions should be taken into account, such as the prompt photon produced by the initial hard scattering, fragmentated photons by jet fragmentation, jet-photon conversion[33], et al. A systematical study will also include other nuclear effects such as Cronin effect, (anti-)shadowing effect and final jet quenching effect for a jet fragmentated into a photon, just like our current studies[13, 34] for high p_T hadrons in $A + A$ collisions. This kind of detailed calculating and analyzing for large transverse momentum photon production will be left for a future’s study.

Acknowledgments

The authors are very grateful to Xin-Nian Wang for helpful discussions. This work was supported by MOE of China under Projects No. IRT0624, No. NCET-04-0744 and No. SRFDP-20040511005, and by NSFC of China under Projects No. 10440420018, No. 10475031 and No. 10635020.

-
- [1] M. Gyulassy and X.-N. Wang, Nucl. Phys. **B420**, 583 (1994); X.-N. Wang, M. Gyulassy and M. Plumer, Phys. Rev. D **51**, 3436 (1995).
- [2] R. Baier, Y. L. Dokshitzer, S. Peigne and D. Schiff, Phys. Lett. **B345**, 277 (1995); R. Baier, Y. L. Dokshitzer, A. H. Mueller, S. Peigne and D. Schiff, Nucl. Phys. **B484**, 265 (1997).
- [3] B. G. Zakharov, JETP Lett. **63**, 952 (1996).
- [4] M. Gyulassy, P. Levai and I. Vitev, Phys. Rev. Lett. **85**, 5535, (2000); M. Gyulassy, P. Levai and I. Vitev, Nucl. Phys. B **594**, 371 (2001).
- [5] M. Gyulassy, I. Vitev and X. N. Wang, Phys. Rev. Lett. **86**, 2537 (2001) [arXiv:nucl-th/0012092].
- [6] I. Vitev and M. Gyulassy, Phys. Rev. Lett. **89**, 252301 (2002) [arXiv:hep-ph/0209161].
- [7] I. Vitev, Phys. Lett. B **639**, 38 (2006) [arXiv:hep-ph/0603010].
- [8] A. Majumder, J. Phys. G **34**, S377 (2007) [arXiv:nucl-th/0702066].
- [9] U. A. Wiedemann, Nucl. Phys. **A690**, 731 (2001).
- [10] E. Wang and X.-N. Wang, Phys. Rev. Lett. **87**, 142301 (2001).
- [11] E. Wang and X.-N. Wang, Phys. Rev. Lett. **89**, 162301 (2002).

- [12] Xin-Nian Wang, Phys. Lett. B **595**, 165 (2004); **579**, 299 (2004); Phys. Rev. C, **70**, 031901 (2004).
- [13] Hanzhong Zhang, J. F. Owens, Enke Wang and Xin-Nian Wang, Phys. Rev. Lett., **98**, 212301 (2007); J. Phys. G, **34**, S801 (2007).
- [14] K. Adcox *et al* [PHENIX Collaboration], Phys. Rev. Lett. **88**, 022301 (2002).
- [15] K. Adcox *et al* [PHENIX Collaboration], Phys. Lett. B **561**, 82 (2003).
- [16] C. Adler *et al* [STAR Collaboration], Phys. Rev. Lett. **89**, 202301 (2002).
- [17] C. Adler *et al* [STAR Collaboration], Phys. Rev. Lett. **90**, 032301 (2003).
- [18] C. Adler *et al* [STAR Collaboration], Phys. Rev. Lett. **89**, 082301 (2003).
- [19] C. Adler *et al* [STAR Collaboration], Phys. Rev. Lett. **90**, 082302 (2003).
- [20] J. Adams *et al*. [STAR Collaboration], Phys. Rev. Lett. **97**, 162301 (2006); A. Adare, *et al*. [PHENIX Collaboration], Phys. Rev. C, **77**, 011901 (2008); arXiv: nucl-ex/0801.4545v1.
- [21] C. Y. Wong, *Introduction to High-Energy Heavy Ion Collisions* (World Scientific, Singapore, 1994).
- [22] J. Jalilian-Marian, K. Orginos and I. Sarcevic, Nucl. Phys. B **700**, 523 (2002); Phys. Rev. C **63**, 041901 (2001).
- [23] S. Jeon, J. Jalilian-Marian and I. Sarcevic, Phys. Lett. B **562**, 45 (2003).
- [24] B. G. Zakharov, JETP Lett. **80**, 1-6 (2004).
- [25] T. Isobe [PHENIX Collaboration], J. Phys. G **34**, S1015 (2007) [arXiv:nucl-ex/0701040].
- [26] P. Arnold, G. D. Moore and L. Yaffe, J. High Energy Phys. **11**, 057 (2001); J. High Energy Phys. **12**, 009 (2001); J. High Energy Phys. **06**, 030 (2002).
- [27] S. Turbide, C. Gale, S. Jeon and G. Moore, Phys. Rev. C **72**, 014906 (2005).
- [28] Ben-Wei Zhang, Enke Wang, Chin. Phys. Lett., Vol. **20**, No.5(2003)639.
- [29] L. D. Landau and I.J.Pomeranchuk, Dokl. Akad. Nauk Ser. Fiz. **92**, 735 (1953); A. B. Migdal, Phys. Rev. **103**, 1811 (1956).
- [30] R. Baier, Y. L. Dokshitzer, A. H. Mueller, S. Peigne and D. Schiff, Nucl. Phys. B **478**, 577 (1996).
- [31] E. Braaten, R. D. Pisarski, Nucl. Phys. B **337**, 569 (1990).
- [32] G. Steman, *An introduction to quantum field theory* (Cambridge University Press, 1993).
- [33] R. J. Fries, B. Muller and D. K. Srivastava, Phys. Rev. Lett. **90**, 132301 (2003) [arXiv:nucl-th/0208001].
- [34] Hanzhong Zhang, Enke Wang, Int. J. Mod. Phys. E **16**: 3185-3192, 2008. Hanzhong Zhang, J. F. Owens, Enke Wang and Xin-Nian Wang, arXiv: 0804.2381.